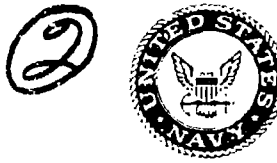


# Naval Research Laboratory

Washington, DC 20375-5000



NRL Memorandum Report 6348

DTIC FILE COPY

## Over-the-Horizon Radar Detection of Targets Via Specular Scatter from Meteor Trails

ROGER O. PILON

*Radar Techniques Branch  
Radar Division*

September 27, 1988

AD-A199 540

STIC  
ELECTED  
OCT 13 1988  
S E D

Approved for public release, distribution unlimited.

88 10 1100 3

## SECURITY CLASSIFICATION OF THIS PAGE

Form Approved  
OMB No 0704-0188

REPORT DOCUMENTATION PAGE			
1a. REPORT SECURITY CLASSIFICATION <b>UNCLASSIFIED</b>		1b. RESTRICTIVE MARKINGS	
2a. SECURITY CLASSIFICATION AUTHORITY		3 DISTRIBUTION/AVAILABILITY OF REPORT Approved for public release; distribution unlimited.	
2b. DECLASSIFICATION/DOWNGRADING SCHEDULE			
4. PERFORMING ORGANIZATION REPORT NUMBER(S) <b>NRL Memorandum Report 6348</b>		5. MONITORING ORGANIZATION REPORT NUMBER(S)	
6a. NAME OF PERFORMING ORGANIZATION <b>Naval Research Laboratory</b>	6b. OFFICE SYMBOL (If applicable) <b>Code 5320</b>	7a. NAME OF MONITORING ORGANIZATION	
6c. ADDRESS (City, State, and ZIP Code) <b>Washington, DC 20375-5000</b>		7b. ADDRESS (City, State, and ZIP Code)	
8a. NAME OF FUNDING / SPONSORING ORGANIZATION <b>ONT</b>	8b. OFFICE SYMBOL (If applicable) <b>ONT 214</b>	9. PROCUREMENT INSTRUMENT IDENTIFICATION NUMBER	
8c. ADDRESS (City, State, and ZIP Code) <b>Arlington, VA 22217</b>		10. SOURCE OF FUNDING NUMBERS	
		PROGRAM ELEMENT NO. <b>6211IN</b>	PROJECT NO <b>RA11A12</b>
		TASK NO	WORK UNIT ACCESSION NO
11. TITLE (Include Security Classification) <b>Over-the-Horizon Radar Detection of Targets Via Specular Scatter from Meteor Trails</b>			
12. PERSONAL AUTHOR(S) <b>Pilon, R.O.</b>			
13a. TYPE OF REPORT <b>Interim</b>	13b. TIME COVERED FROM _____ TO _____	14. DATE OF REPORT (Year, Month, Day) <b>1988 September 27</b>	15. PAGE COUNT <b>20</b>
16. SUPPLEMENTARY NOTATION			
17. COSATI CODES		18. SUBJECT TERMS (Continue on reverse if necessary and identify by block number) <b>Over-the-horizon radar detection of targets Via specular scatter from meteor trails</b>	
FIELD	GROUP	SUB-GROUP	
19 ABSTRACT (Continue on reverse if necessary and identify by block number)			
<p>The use of specular scatter from ionized meteor trails for over-the-horizon communications, known as meteor burst communications, has been studied for its applicability to over-the-horizon radar detection of targets. The high propagation losses associated with meteor trails scattering in general require transmitter power-antenna gain products, in excess of 100 dBW, for modest target detection capabilities. Most of the target detection capabilities of meteor trail scattering are available using high-frequency over-the-horizon radar, which generally offers better signal-to-noise ratios and a superior rate of detection. The reradiation pattern of an ionized meteor trail and its unknown orientation combine to introduce extraordinary ambiguities in the target's location with respect to both ground range and azimuthal direction.</p>			
20. DISTRIBUTION/AVAILABILITY OF ABSTRACT <input checked="" type="checkbox"/> UNCLASSIFIED/UNLIMITED <input type="checkbox"/> SAME AS RPT <input type="checkbox"/> DTIC USERS		21. ABSTRACT SECURITY CLASSIFICATION <b>UNCLASSIFIED</b>	
22a. NAME OF RESPONSIBLE INDIVIDUAL <b>R.O. Pilon</b>		22b. TELEPHONE (Include Area Code) <b>(202) 767-4873</b>	22c. OFFICE SYMBOL <b>Code 5320</b>

## CONTENTS

INTRODUCTION .....	1
THE PROPAGATION GEOMETRY .....	1
METEOR TRAIL CROSS SECTIONS .....	2
POWER-GAIN REQUIREMENTS .....	4
THE RATE OF DETECTION .....	10
POWER AND SIGNAL-TO-NOISE COMPARISONS .....	10
OBJECT POSITION AMBIGUITIES .....	13
CONCLUSIONS .....	14
REFERENCES .....	14
BIBLIOGRAPHY .....	14
APPENDIX .....	17

Accession For	
NTIS GRA&I	
DTIC TAB	
Unannounced <input type="checkbox"/>	
Justification	
By _____	
Distribution/ _____	
Availability Codes	
Dist	Avail and/or
	Special
A-1	



## OVER-THE-HORIZON RADAR DETECTION OF TARGETS VIA SPECULAR SCATTER FROM METEOR TRAILS

### INTRODUCTION

Each day approximately  $10^{10}$  to  $10^{12}$  meteors enter the earth's atmosphere and produce ionized trails that are useful in VHF communications. This form of communications, known as meteor burst communications, exploits specular scatter from the short lived but abundant ionized trails to transfer bursts of data between distant installations. The subject of this report is the applicability of this type of scatter for over-the-horizon radar detection of targets. The propagation geometry, the radar cross section of meteor trails, the transmitter power-antenna gain requirements for the radar system, the rate of detection, power and signal-to-noise comparisons, and target position ambiguities are discussed in this report. Some of the pertinent aspects of meteor trails are reviewed in the appendix.

### THE PROPAGATION GEOMETRY

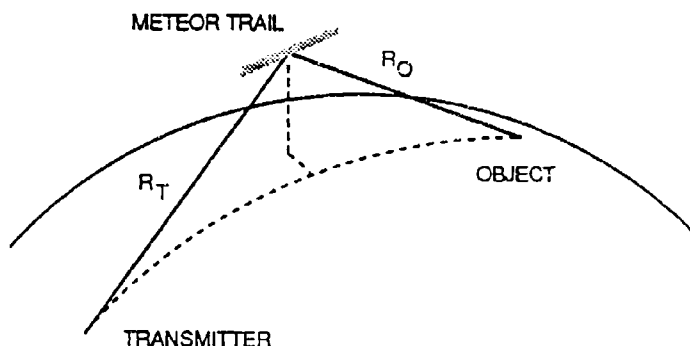


Fig. 1. The geometry for specular radar scatter from a meteor trail.

The geometry for the radar detection of an object via specular scatter from a meteor trail is indicated in Fig. 1, where  $R_T$  is the distance from the transmitter to the meteor trail and  $R_O$  is the distance from the meteor trail to the object (target). Assuming a meteor trail altitude of 100 km and considering the curvature of the earth and the refraction of the radar beam, the maximum distance  $R_T + R_O$  is about 2600 km (1400 nmi). The condition for specular scatter is that the angle between the incident path of propagation and the axis of the trail must be equal to the angle between the scattered path of propagation and the axis of the trail. This condition is satisfied if

the axis of the trail lies in a plane tangent to an ellipsoid whose foci are at the transmitter and the object. The scattered power for a non-specular scatter is very low compared to that for a specular scatter.

If the transmitted energy is directed along the azimuth of the great circle path to the object, the probability of detection is small. This is particularly true for long ranges where  $R_T \approx R_O$ . since the probability of a meteor traveling parallel to the earth's surface is low. This also applies, but to a lesser extent, at shorter ranges. If the flux of meteors incident on the earth's path through space were isotropic, the azimuths for the most probable detection would, on average, be the azimuth of the great circle path plus and minus approximately seven degrees. However, the actual distribution is such that the azimuth to a detected object is, on average, the azimuth of the transmitted energy plus and minus about fifteen degrees. The departures from this average distribution are due to the latitude and direction of propagation with respect to the ecliptic, the time of day and the month of the year.

For a transmitter power  $P_T$  and antenna gain  $G_T$ , the power density at the object is

$$\frac{P_T G_T}{4\pi R_T^2} \sigma_{t1} \frac{1}{4\pi R_O^2} . \quad (1)$$

where  $\sigma_{t1}$  is the radar scattering cross section of the meteor trail for the propagation path from the transmitter to the object. The return path via the same meteor trail produces a power density at the receiver that is equal to the above quantity multiplied by

$$\sigma_0 \frac{1}{4\pi R_O^2} \sigma_{t2} \frac{1}{4\pi R_T^2} . \quad (2)$$

where  $\sigma_0$  is the cross section of the object and  $\sigma_{t2}$  is the scattering cross section of the meteor trail for the return path. Since the capture area of the receiving antenna is

$$A_c = \frac{G_R \lambda^2}{4\pi} . \quad (3)$$

where  $G_R$  is the gain of the receiving antenna and  $\lambda$  is the radar wavelength, the received power is

$$P_R = \frac{P_T G_T G_R \lambda^2 \sigma_{t1} \sigma_{t2} \sigma_0}{1024\pi^5 R_T^4 R_O^4} . \quad (4)$$

## METEOR TRAIL CROSS SECTIONS

The scattering cross sections for underdense and overdense meteor trails have been derived by Eshleman [1] and reviewed by Sugar [2]. Cross section, as defined by Sugar, is the ratio of the power scattered per unit solid angle to the power incident per unit area. This definition is  $(1/4\pi)$  times the generally accepted definition, which is the ratio of the power scattered into  $4\pi$  steradians to the power incident per unit area. Therefore, the cross sections indicated by Sugar will be multiplied by  $4\pi$ .

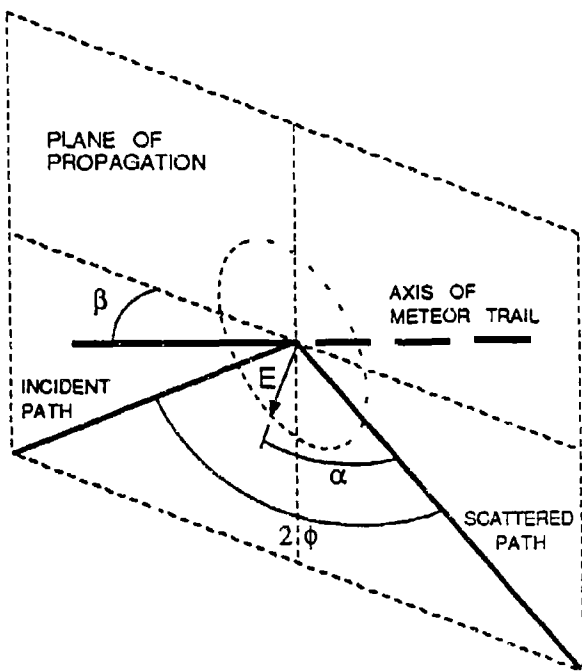


Fig. 2. The scattering geometry at the meteor trail.

For an underdense meteor trail

$$\sigma_{t_0} = \frac{4\pi R_T R_O \lambda r_e^2 q^2 \sin^2 \alpha}{(R_T + R_O)(1 - \cos^2 \beta \sin^2 \phi)} e^{-\frac{8\pi^2 r_o^2}{\lambda^2 \sec^2 \phi}} e^{-\frac{32\pi^2 D_u}{\lambda^2 \sec^2 \phi} \tau} . \quad (5)$$

where  $r_e$  is the classical radius of the electron ( $2.8178 \times 10^{-15}$  m),  $q$  is the electron line density of the trail in electrons per meter,  $r_o$  is the initial radius of the trail,  $D_u$  is the diffusion coefficient of the underdense trail, and  $\tau$  is the time measured from the formation of the trail. As shown in Fig. 2,  $\alpha$  is the angle between the electric vector incident on the trail and the scattered path,  $\beta$  is the angle between the axis of the meteor trail and the plane of the incident and scattered paths, and  $\phi$  is one-half the included angle between the incident and scattered paths.

As the trail forms its cross section increases rapidly to a magnitude determined in part by  $r_o$ , the initial radius of the trail, after which it decays exponentially as the electrons diffuse into the surrounding atmosphere. A "maximum" cross section may be considered to be that determined by only the first term in Eq. (5), i.e.  $r_o = \tau \approx$  zero.

For an overdense meteor trail

$$\sigma_{t_0} = \frac{4\pi R_T R_O \sin^2 \alpha}{(R_T + R_O)(1 - \cos^2 \beta \sin^2 \phi) \sec \phi} [D_o \tau \ln(r_o q \lambda^2 \sec^2 \phi / 4\pi^2 D_o \tau)]^{1/2} . \quad (6)$$

where  $D_o$  is the diffusion coefficient for the overdense trail.

The cross section of an overdense trail rises and falls with time  $\tau$  with a shape similar to an inverted U. The cross section reaches a maximum at

$$\tau_{\max} = \frac{r_e q \lambda^2 \sec^2 \phi}{4\pi^2 D_o e} . \quad (7)$$

where  $e$  is the base of the natural logarithm. Thus,

$$\max \sigma_{t_0} = \frac{2e^{-1/2} R_T R_O \lambda r_e^{1/2} q^{1/2} \sin^2 \alpha}{(R_T + R_O)(1 - \cos^2 \beta \sin^2 \phi)} . \quad (8)$$

The "maximum" cross sections of both underdense and overdense meteor trails are equal for an electron line density of  $q = 0.7468 \times 10^{14}$  electrons/m. Therefore,

$$\max \sigma_t = \frac{0.5565 R_T R_O \lambda \sin^2 \alpha}{(R_T + R_O)(1 - \cos^2 \beta \sin^2 \phi)} \left| \frac{q}{0.7468 \times 10^{14}} \right|^{\kappa} . \quad (9)$$

where  $\kappa = 2$  for an underdense trail and  $1/2$  for an overdense trail. The generally accepted demarcation between underdense and overdense trails remains in the range  $1-2.4 \times 10^{14}$  electrons/m.

## POWER-GAIN REQUIREMENTS

Combining Eqs. (4) and (9),

$$\max P_R = \frac{(P_T G_T G_R) \lambda^4 \sigma_0}{3307 \pi^5 R_T^2 R_O^2 (R_T + R_O)^2} \frac{\sin^2 \alpha_1 \sin^2 \alpha_2}{(1 - \cos^2 \beta \sin^2 \phi)^2} \left| \frac{q}{0.7468 \times 10^{14}} \right|^{2\kappa} . \quad (10)$$

where the subscripts 1 and 2 refer to the quantities for the propagation path from the transmitter to the object and the return path from the object to the receiver, and, since the same meteor trail is utilized for both paths,  $\beta_1 = \beta_2 = \beta$  and  $\phi_1 = \phi_2 = \phi$ .

The received power is a function of the available transmitter power-antenna gain product  $P_T G_T G_R$ . While a primary site for the deployment of a target detection radar utilizing meteor trail scatter is on a ship, which would be able to generate copious amounts of transmitter power, the size, and gain, of the antennas that may be used would be restricted. For instance, a phased array antenna of dimensions 10 m by 20 m, operating at 50 MHz, would have a one-way gain of 18.5 dB. For a peak transmitter power of one megawatt, the power-gain product would be 97 dBW.

Another antenna configuration might employ half-wave dipoles positioned along the mast of the ship as a transmitter and quarter-wave monopoles positioned along the periphery of the hull to function as the receiver. A typical mast height of 45 m could accommodate a linear array of 14 half-wave dipoles, yielding a gain in the horizontal direction of 19.6 dB when the image of the antenna in the ocean surface is included. To illuminate all azimuths, three such arrays may be used, placed at 120 degree intervals around the mast. For a ship that is 120 m long approximately 40 quarter-wave monopoles may be placed along each side of the hull. The endfire and broad-

side gain in the horizontal direction for each of these two arrays would be 21.2 dB. For this configuration and a peak transmitter power of one megawatt, the power-gain product would be 101 dBW.

A currently and practically realizable power-gain product from the standpoint of available power and antenna design is thus about 100 dBW. The minimum power-gain product required for target detection, based on propagation and receiver noise parameters, may be obtained by rewriting Eq. (10) as

$$\min(P_T G_T G_R) = \frac{3307\pi^5 P_R}{\lambda^4 \sigma_0} Q^{-2\kappa} F^{-1}. \quad (11)$$

where the first term encompasses the necessary parameters of the radar system and the target,

$$Q = \frac{q}{0.7468 \times 10^{14}} \quad (12)$$

is the normalized electron line density of the meteor trail, and

$$F = \frac{\sin^2 \alpha_1 \sin^2 \alpha_2}{R_T^2 R_O^2 (R_T + R_O)^2 (1 - \cos^2 \beta \sin^2 \phi)^2} \quad (13)$$

encompasses all of the geometrical factors of propagation and scattering.

As an example, assume that the radar is operating at a frequency of 50 MHz with a noise power of -180 dBW. If an object with a cross section of 20 dBm<sup>2</sup> is to be detected with a S/N of 13 dB, the minimum power-gain requirement is

$$\min(P_T G_T G_R) = \frac{1.012 \times 10^6 \cdot 10^{-16.7} W}{(6m)^4 \cdot 100 m^2} Q^{-2\kappa} F^{-1} \quad (14)$$

$$= [-158.1 - 2\kappa Q - F] \text{ dBW} \quad (15)$$

where  $Q = 10 \log Q$  and  $F = 10 \log F$  if the ranges are expressed in meters.

The factor F is plotted in Figures 3 through 9. These plots are for a meteor trail altitude of 100 km and for angles  $\alpha_1$  and  $\alpha_2$  of 90°. The latter assumption is roughly valid for all polarizations at the longer ranges and for horizontally polarized energy incident on the meteor trail for short ranges. However, due to Faraday rotation in the ionosphere, the polarization of the radar energy incident on the meteor trail is unknown. Thus, these are maximum values with respect to polarization considerations. The abscissa of each plot spans the ground range in kilometers to the nadir of all meteor trails capable of scattering the radar beam to the object and then back to the transmitter-receiver. Positive ranges are directed from the transmitter toward, and past, the object. Negative ranges are directed in the opposite direction. In Figures 4 through 6 the transmitter is represented by the square on the abscissa to the left of center and the object is represented by the square to the right of center. The ground range at the mid-point of the abscissa is half-way between the transmitter and the object. Thus, the seven Figures are for transmitter-object ground range separations of 0, 100, 500, 1000, 1500, 2000 and 2500 km. Fig. 3, for a transmitter-object separation of zero, is intended to approximate the factor F for an object somewhere in the two dimensional area near the transmitter.

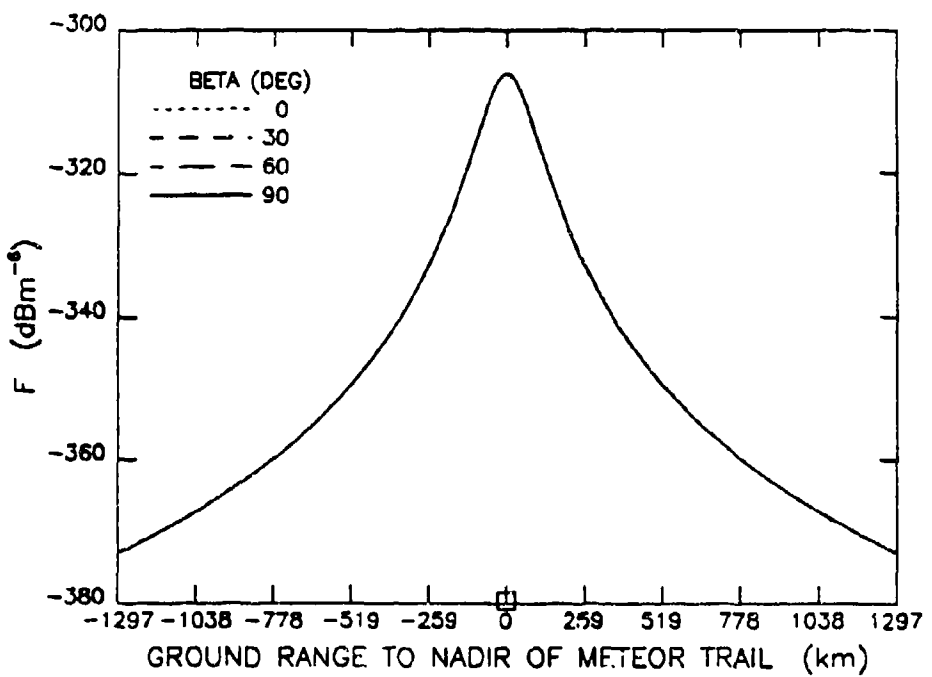


Fig. 3. The factor  $F$  for an object in the vicinity of the transmitter.

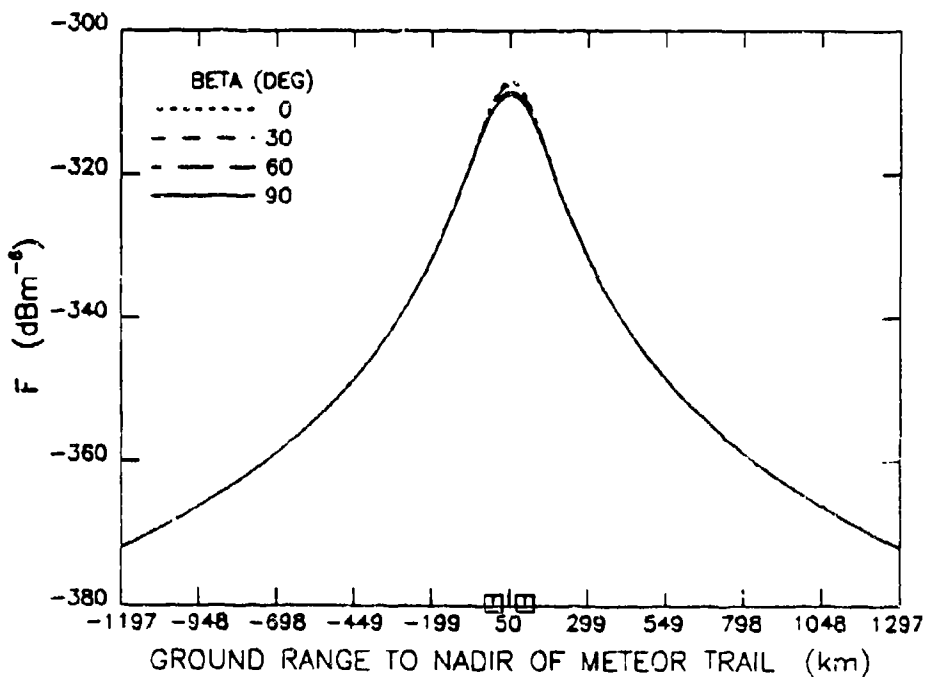


Fig. 4. The factor  $F$  for an object 100 km from the transmitter.

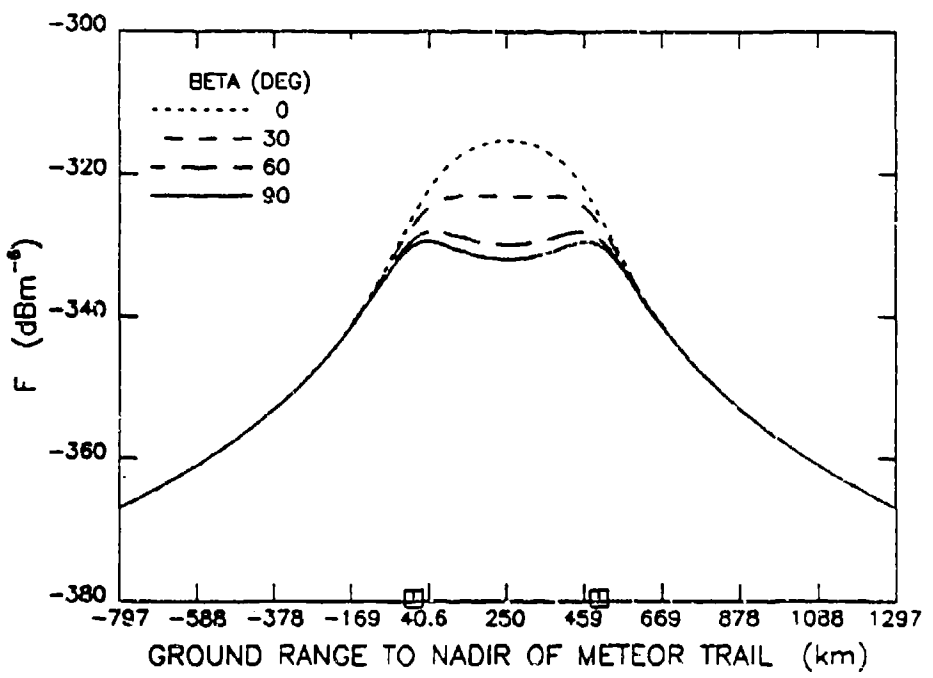


Fig. 5. The factor  $F$  for an object 500 km from the transmitter.

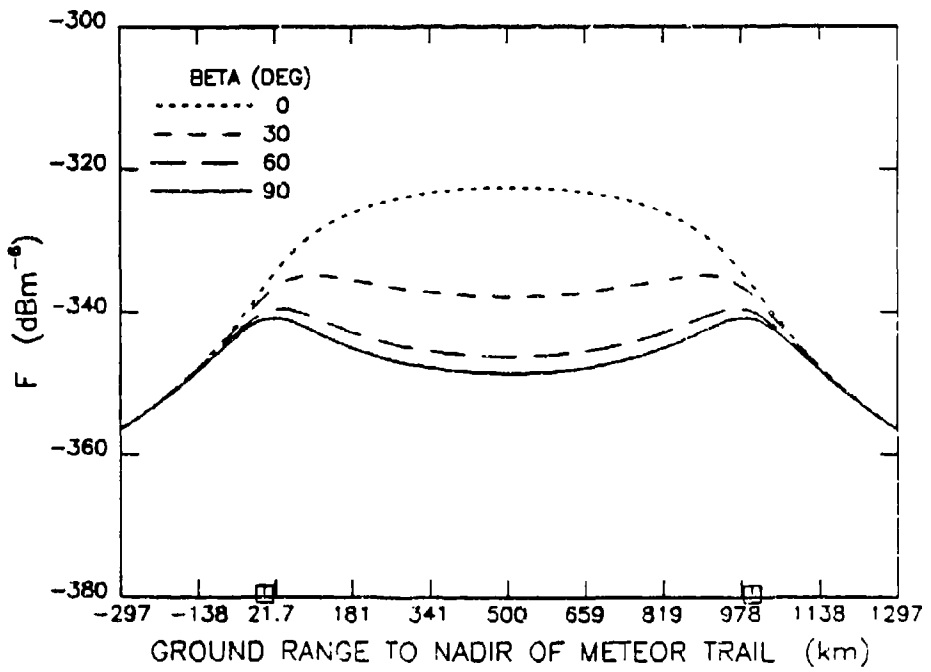


Fig. 6. The factor  $F$  for an object 1000 km from the transmitter.

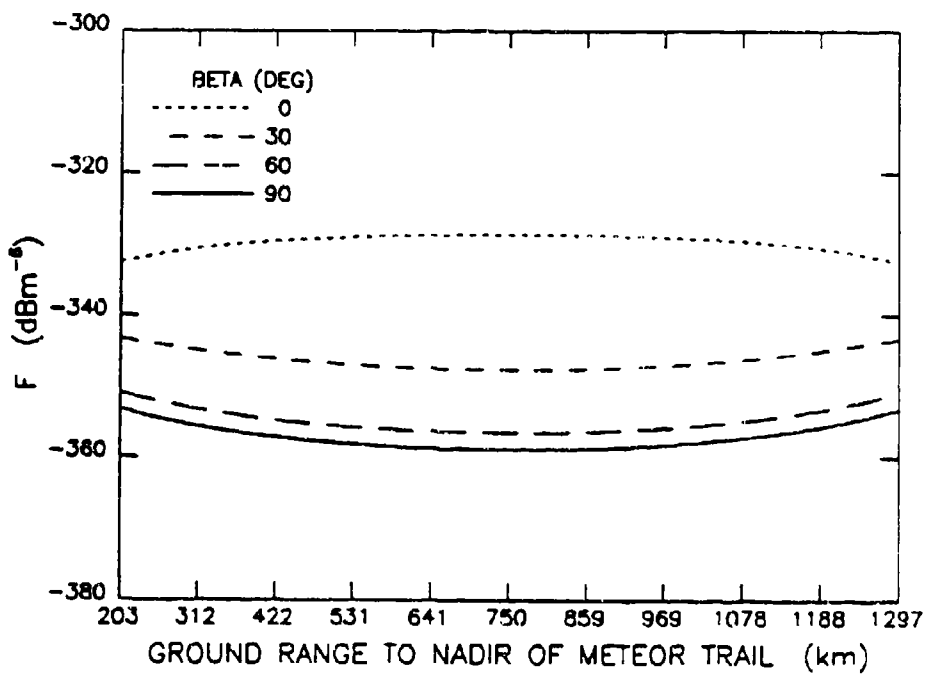


Fig. 7. The factor  $F$  for an object 1500 km from the transmitter.

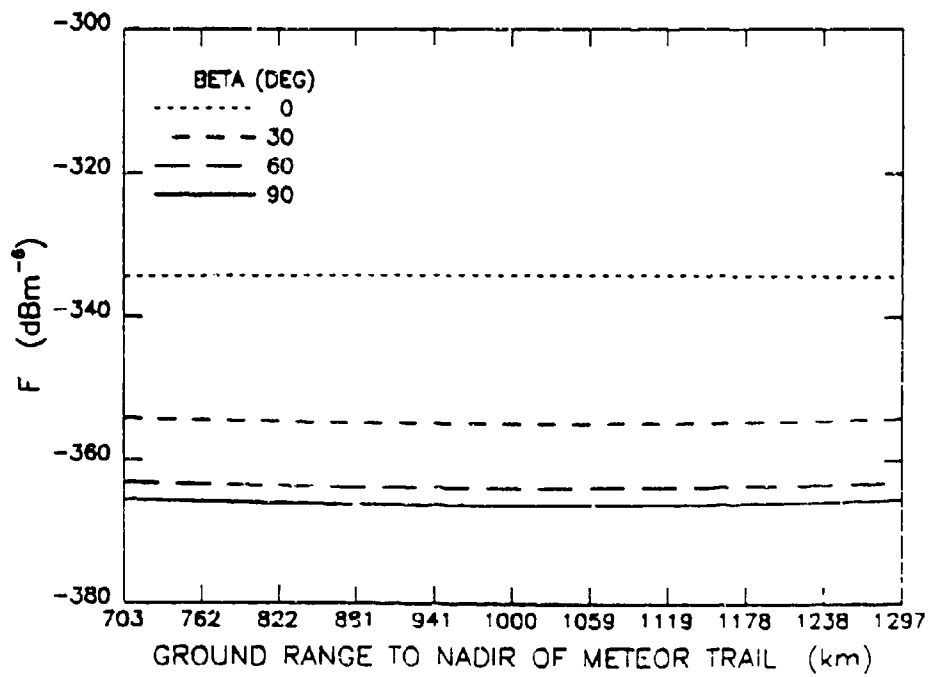


Fig. 8. The factor  $F$  for an object 2000 km from the transmitter.

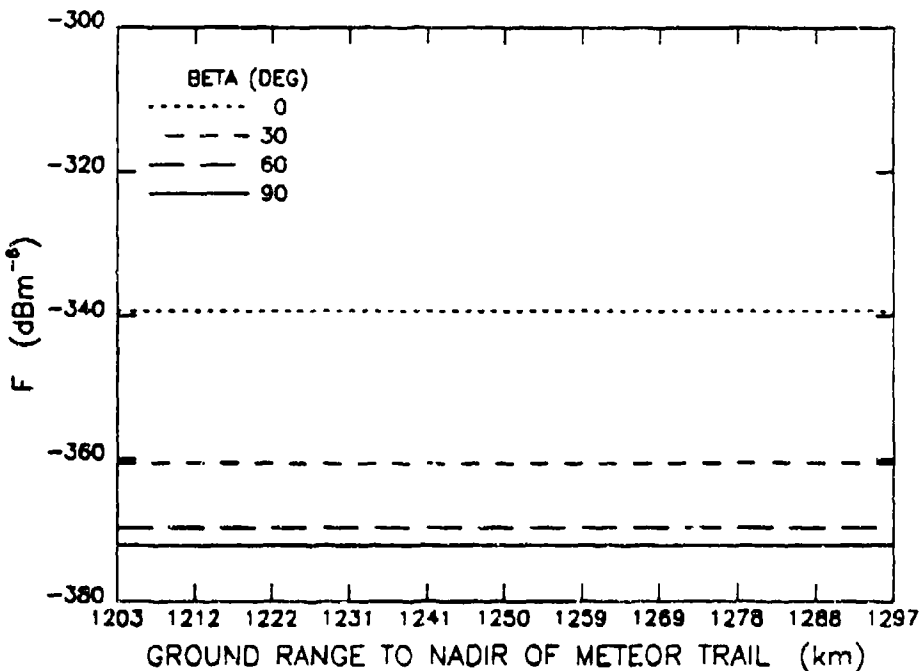


Fig. 9. The factor F for an object 2500 km from the transmitter.

For a transmitter-object separation of 100 km the maximum value of F is  $-307 \text{ dBm}^{-6}$ . Assuming an available power-gain product of 100 dB, a meteor trail with an electron line density of about  $6 \times 10^{18}$  electrons per meter would be required to detect a  $20 \text{ dBm}^2$  object with a S/N of 13 dB. The occurrence of such an extremely overdense trail is rare, and thus the probability of detection of the object, even at the short actual range of 100 km, would be very low. This result is based on the requirements for detection by a single pulse. If the one megawatt peak power transmitter is operating at an average power of 100 kW with a pulse length of 5 microseconds,  $6 \times 10^4$  individual pulses could be integrated over a trail lifetime of three seconds. This would effectively increase the available power-gain product by 48 dB. Assuming an underdense meteor trail lifetime of three seconds, the radar cross section of the trail would decrease to  $e^{-1}$  of its initial value over that period, reducing the effective increase to 44 dB. Thus, a properly oriented meteor trail of  $2.4 \times 10^{14}$  electrons per meter would allow detection of the object. This electron line density is at the upper limit for an underdense meteor trail, justifying the assumption of a trail lifetime of about three seconds.

The maximum attainable value of F for a meteor trail height of 100 km is  $-306 \text{ dBm}^{-6}$ , as shown in Fig. 3. Thus, the above case represents very nearly a (theoretical) best case. It is seen in Figures 5 through 9 that the values for F decrease with increasing transmitter-object separation, and, at any given separation, that the variation in F with beta increases. The former indicates that the transmitter power-antenna gain-processing gain product would have to increase with increasing separation (all other factors being equal) and the latter indicates that a greater range of received power levels would have to be acceptable if all sufficiently oriented trails are to be useful. Otherwise, the rate of detection of the object would decline.

## THE RATE OF DETECTION

For normal meteor burst communications, which utilizes both underdense and overdense meteor trails and all trail orientation angles beta, the average time between suitable bursts is about 20 seconds. The average burst length is about 0.2 to 0.4 seconds. This may indicate that the bulk of meteor burst communications occur via trails of approximately  $2 \times 10^{13}$  electrons per meter. On this basis, the time between detections of an object would average [ $q / (2 \times 10^{13})$ ] times 20 seconds, where  $q$  is the minimum trail density that would allow the detection. For the example discussed above, where an electron line density of  $2.4 \times 10^{14}$  yielded detectability, the average rate of detection would be once every four minutes. Yearly and diurnal variations in the rate of occurrence of meteor trails would indicate a range of from more than 0.67 detections per minute to less than 0.033 detections per minute, i.e. more than 30 minutes per detection. If the available power-gain product can be increased by a few tens of decibels, the rate of detection can become acceptable for the short transmitter-object ground range of 100 km.

As the ground range increases, much of any possible increase in the available power-gain product would be required to increase the object's power return to an acceptable level. Further increases in the available power-gain product could then contribute to increasing the rate of detection. Also, in Figures 5 through 9 it is seen that the variation in F with beta can be substantial. If the requirements on the received power are such that only trails oriented at an angle beta significantly less than  $90^\circ$  are sufficient, this decrease in the set of acceptable meteor trail orientations decreases the rate of detection of the object.

## POWER AND SIGNAL-TO-NOISE COMPARISONS

Normal meteor burst communications are conducted for ground ranges far greater than 100 km and at power-gain products much less than the 100 dBW discussed above. The additional propagation loss from the return path accounts for the difference. If a receiving antenna of gain  $G_O$  is placed at the position of the object, the received power  $P_O$  is

$$P_O = \frac{P_T G_T G_O \lambda^2 \sigma_{t1}}{64\pi^3 R_T^2 R_O^2} . \quad (16)$$

This would be the received power for normal meteor burst communications. Starting with Eq. (4) for  $P_R$ , assuming that  $G_O$  is equal to  $G_R$ , and that  $\sigma_0 = 10 \log [\sigma_O (\text{m}^2)]$ , the ratio of the received power at the transmitter-receiver,  $P_R$ , to  $P_O$  is

$$\frac{P_R}{P_O} = [ -16.75 + 0.5 F + \kappa Q + \sigma_0 ] \text{ dB} \quad (17)$$

for a radar frequency of 50 MHz. For the parameters discussed above, an underdense trail with an electron line density of  $2.4 \times 10^{14}$  electrons per meter and an average of one detection every four minutes,  $\kappa Q = 10$  dB. Since the maximum value for F is  $-306 \text{ dBm}^{-6}$ .

$$\left[ \frac{P_R}{P_O} \right]_{\max} = [ -160 + \sigma_0 ] \text{ dB} . \quad (18)$$

Even for an extremely short ground range and a large object cross section of  $\sigma_0 = 40 \text{ dBm}^2$ ,  $P_R$  is extremely low compared to  $P_O$ .

Most of the over-the-horizon target detection capabilities of meteor burst scattering at VHF frequencies (VHF-MB) are available using high-frequency over-the-horizon (HF-OTH) radar. A pertinent question for a ship board or any other installation is: For a given available transmitter power and antenna capture area, which system would provide the greatest S/N for a given target?

The received power for an HF-OTH system operating in the skywave mode is

$$P_R = \frac{P_T G_T G_R \lambda^2 \sigma_0}{64\pi^3 R^4 L} , \quad (19)$$

where  $R$  is the radar range,  $L$  (greater than 1) accounts for losses such as absorption and transmission through the ionized layers, and, as in Eqs. (4) and (10),  $G_T$ ,  $G_R$ ,  $\lambda$  and  $\sigma_0$  vary with the radar operating frequency. The ratio of the received powers for the two systems may be reduced to

$$\frac{P_R(\text{VHF-MB})}{P_R(\text{HF-OTH})} = 0.001961 R^4 L \lambda_{OTH}^2 F Q^{2K} \frac{\sigma_{O_{MB}}}{\sigma_{O_{OTH}}} . \quad (20)$$

In terms of the geometrical factors of propagation and scattering, the maximum return for the meteor burst system occurs when the meteor trail's nadir is midway between the transmitter and the object,  $\beta = 0^\circ$ , and  $\alpha_1 = \alpha_2 = 90^\circ$ . For these conditions,

$$F_{\max} = \frac{16}{R^6 (1-\sin^2\phi)^2} \quad (21)$$

Eq. (20) then becomes, in decibel form.

$$\frac{P_R(\text{VHF-MB})}{P_R(\text{HF-OTH})} = [-19.05 + 0.3333 F_{\max} + 0.6667 \Delta F + 2 \kappa Q + L + 2 \Lambda_{OTH} + \Xi_O] \text{ dB} . \quad (22)$$

where  $(1-\sin^2\phi)^{-2}$  becomes  $\Delta F$ , which is equal to  $F(\beta=0^\circ) - F(\beta=90^\circ)$  midway between the transmitter and the object,  $L = 10 \log R$ ,  $\Lambda_{OTH} = 10 \log \lambda_{OTH}$ , and  $\Xi_O = 10 \log (\sigma_{O_{MB}} / \sigma_{O_{OTH}})$ .

Assuming an average loss  $L$  of 15 dB, a  $\Xi_O$  of +12 dB per frequency octave and an environmental noise of  $[-148 - 12.6 \ln(f_{MHz}/3)] \text{ dBW}$ , or -8.73 dBW per frequency octave, the ratios of the S/N are given in TABLE I for ground ranges of 500, 1000 and 2500 km, at four HF-OTH frequencies. The ratios of the S/N for meteor burst propagation with respect to the S/N for HF-OTH groundwave propagation are also presented in TABLE I, for ground ranges of 50, 100 and 200 km. Representative losses for groundwave propagation have been used and it has been assumed that the cross section of the object for energy incident parallel to the earth's surface is 25 dB lower than that for the higher elevation angles encountered with meteor burst scattering.

All of the ratios in TABLE I are dependent on the electron line density of each meteor trail through the quantity  $2\kappa Q$ . For an underdense trail with an electron line density of  $2.4 \times 10^{14}$  electrons per meter, yielding an average of one detection every four minutes,  $2\kappa Q = 20 \text{ dB}$ . All trails with a higher electron line density would be considered overdense, for which  $\kappa = 1/2$  instead of 2.

TABLE I

$$\frac{S}{N} \text{ (VHF-MB)}$$


---


$$\frac{S}{N} \text{ (HF--OTH)}$$

HF MODE	GROUND RANGE (km)	HF-OTH RADAR FREQUENCY (MHz)			
		3	7.5	15	30
GROUNDWAVE	50	-9 + 2kQ	-39 + 2kQ	-59 + 2kQ	-59 + 2kQ
	100	5 + 2kQ	-23 + 2kQ	-36 + 2kQ	-23 + 2kQ
	200	22 + 2kQ	1 + 2kQ	0 + 2kQ	31 + 2kQ
SKYWAVE	500	25 + 2kQ	-9 + 2kQ	-36 + 2kQ	-63 + 2kQ
	1000	29 + 2kQ	-5 + 2kQ	-32 + 2kQ	-59 + 2kQ
	2500	28 + 2kQ	-6 + 2kQ	-33 + 2kQ	-60 + 2kQ

VHF-MB RADAR FREQUENCY: 50 MHz

It should be noted that the ratios presented in TABLE I assume optimum conditions for meteor trail scattering and only average conditions for HF-OTH operation. The ratios assume an instantaneous maximum scattered power for  $r_s = r = 0$  for an underdense trail, or a maximum scattered power for an overdense trail. Integrating the received power over the lifetime of the trail would decrease the ratios by a few dB. It has been assumed that  $\alpha_1 = \alpha_2 = 90^\circ$ . Even for the optimum object ground ranges, the polarization of the energy incident on the meteor trail varies due to Faraday rotation. On a trail-to-trail basis, the reduction in the ratios could vary from near 0 dB to tens of dB. Also, the optimum location of the trail, midway between the transmitter-receiver and the object, and orientation,  $\beta = 0^\circ$ , have been assumed. For other locations or orientations the ratios could decrease by tens of dB. In addition, the power received via meteor trail scattering can only be integrated over the life of each individual trail. For HF-OTH propagation, however, the detection is nearly continuous and the received power may be integrated over a longer period. The increased processing gain available for an HF-OTH system would further decrease the ratios given in TABLE I.

TABLE I therefore indicates that, on average, the S/N for a meteor burst system may be equal or superior to that for an HF-OTH system operating at 3 MHz and ranges of 200 km or greater, or at 30 MHz and 200 km. The two major reasons for the possibly equal or superior performance of the meteor burst system at 3 MHz are the low cross section of the object at 3 MHz relative to that at 50 MHz, and the higher environmental noise at 3 MHz relative to 50 MHz. The relative performance of the meteor burst system degrades rapidly with increasing HF-OTH radar frequency, except for groundwave propagation near the high end of the band. This is due to an increasing loss for groundwave propagation as the frequency increases. The possibly superior per-

formance of a meteor burst system relative to an HF-OTH system at 30 MHz and 200 km is due to a combination of the increasing loss for groundwave propagation at the higher frequencies and the longer range.

TABLE I indicates that over the majority of the HF-OTH frequency band and object ranges, an HF-OTH system would yield superior S/N relative to a meteor burst system. It would also allow nearly continuous surveillance of a target, whereas the rate of detection for a meteor burst system would be relatively low.

## OBJECT POSITION AMBIGUITIES

In normal meteor burst communications the azimuth of the most probable path, on average, is that of the great circle direction to the installation  $\pm 15^\circ$ . This would also apply to the present discussion. In addition there are other ambiguities, as evidenced by Figures 3 through 9. In Figures 3 through 6 it is seen that propagation paths exist for meteor trails beyond the object and even in the opposite direction. Thus, object position determinations based on the propagation time delay and the transmission-reception direction are ambiguous. While the received power for the more grossly ambiguous positions declines rapidly in Figures 3 and 4, Figures 5 and 6 show significant expanses in range where the variation in received power would be relatively small.

Other examples of object position ambiguity are also evident. Assume a transmitter-object separation of 500 km, i.e. Fig. 5. For a meteor trail midway between the two and oriented to provide a specular path with  $\beta = 90^\circ$ , the factor F is  $-332 \text{ dBm}^{-6}$ . If another object is near the transmitter (approximated by a zero km separation, Fig. 3), the factor F for the same meteor trail - 250 km from the transmitter - is also  $-332 \text{ dBm}^{-6}$ . Thus, the object could be at a ground range of 500 km in a (roughly) known direction or it could be near the transmitter in an unknown direction. This same ambiguity can also exist for other meteor trail orientations. For example, for  $\beta = 0^\circ$  the factor F in Fig. 5 is  $-315 \text{ dBm}^{-6}$ . If the angle of descent of the meteor were to be much steeper, providing a specular path back to the vicinity of the transmitter instead of the assumed object ground range of 500 km, and the radar cross section of the nearby object were  $17 \text{ dBm}^2$  greater than that of the distant object, the received power would be the same. This type of ambiguity occurs because the orientation and electron line density of any given meteor trail, as well as the incident polarization and radar cross section of the object, are unknown.

A similar situation exists for  $\beta = 60^\circ$  in Fig. 5 with respect to a transmitter-object separation of 100 km (Fig. 4), where the values for F are  $-330$  and  $-328 \text{ dBm}^{-6}$ . A difference in the propagation time delay would also exist in this latter case, but if the height of the meteor trail or the radar cross sections are unknown, or if propagation losses and/or polarizations are variable, as they generally are, the ambiguity would not be resolvable.

These types of ambiguities exist for all transmitter-object separations. Consider a transmitter-object separation of 2500 km (Fig. 9). The value of F for  $\beta = 90^\circ$  is  $-372 \text{ dBm}^{-6}$ . In Fig. 3, for a trail ground range of 1250 km, the value of F is also  $-372 \text{ dBm}^{-6}$ . Thus, the object being detected could be at a ground range of 2500 km or it could be near the radar system. If the nearby object is larger in radar cross section than the distant object, the received power levels would be similar for other meteor trail orientations.

In the above examples only the most probable paths have been considered, i.e. paths utilizing meteor trails near a reference plane defined by the great circle through the transmitter-receiver and the object and the center of the earth. Actually, a three dimensional surface describes the probability distribution of properly oriented meteor trails, with significant extent on both sides of the reference plane. Therefore, the factor F would define a three dimensional surface, decreasing monotonically with distance measured perpendicular to the reference plane. The values for F

shown in Figures 3 through 9 are only those along the intersection of the surface with the reference plane. Hence, many other ambiguities in azimuthal direction and range also exist.

## CONCLUSIONS

The received power levels for over-the-horizon radar detection of targets via meteor trails are very low, leading to requirements for high available transmitter power-antenna gain-processing gain products. It has been shown that a  $20 \text{ dBm}^2$  target at a ground range of 100 km can be detected at an acceptable rate. However, at longer ranges any increase in the available power-gain product would have to be apportioned between the power requirements for detectability and the requirements to utilize trails of lesser electron line densities and of a significant range of orientations to increase to rate of detection.

At any given point on the earth's surface the rate of occurrence of meteor trails varies by a factor of four throughout a 24 hour day and by a factor of five throughout the year. Thus, a consideration in the system design would be the minimum acceptable rate of detection, necessitating an increase in the available power-gain product of more than 9 dB over that based on average rates of detection.

For a given available transmitter power and antenna capture area, an HF-OTH system operating in the skywave and groundwave modes offers superior S/N ratios over most of the HF-OTH frequency band, relative to a meteor burst system. In addition, an HF-OTH system allows nearly continuous surveillance of a target, whereas the rate of detection for a meteor burst system is relatively low.

The ambiguities in establishing the position of a detected target are significant. If the available power-gain product is limited to the point where only a shorter range target can be detected, its azimuthal direction can be estimated only if its range is known apriori. The propagation delay via a meteor trail of relatively unknown position does not, in general, establish the range well enough to determine the target's direction to better than an estimated plus or minus one quadrant in azimuth. As the available power-gain product increases, the error in the direction to a shorter range target increases, as does the error in the actual ground range to the target. The range error continues to increase with transmitter-target separation but the directional ambiguity decreases for separations nearing 2600 km.

## REFERENCES

1. V.R. Eshleman, in *The Radio Noise Spectrum*, D.H. Menzel, ed., (Harvard University Press, Cambridge, Massachusetts, 1960), Ch. 4.
2. G.R. Sugar, "Radio Propagation by Reflection from Meteor Trails," Proceedings of the IEEE 52, 116-136 (February 1964).

## BIBLIOGRAPHY

1. Akram, F., N.M. Sheikh, A. Javed, and M.D. Grossi, "Impulse Response of a Meteor Burst Communications Channel Determined by Ray-Tracing Techniques," IEEE Transactions on Communications COM-25(4), 467-470 (April 1977).
2. Brown, D.W., "A Physical Meteor-Burst Propagation Model and Some Significant Results for Communication System Design," IEEE Journal on Selected Areas in Communications, SAC-3(5), 745-755 (September 1985).

3. Canon, P.S., "Polarization Rotation in Meteor Burst Communication Systems," *Radio Science* 21(3), 501-510 (May-June 1986).
4. Morgan, E.J., "The Resurgence of Meteor Burst," *Signal* 37(5), 69-73 (January 1983).
5. Oetting, J.D., "An Analysis of Meteor Burst Communications for Military Applications," *IEEE Transactions on Communications COM-28(9)*, 1591-1601 (September 1980).
6. Richmond, R.L., "Meteor Burst Communications, Part I: MBC Advances Assist C<sup>3</sup> Objectives," *Military Electronics/Countermeasures* 8(8), 68-72 (August 1982).
7. Richmond, R.L., "Meteor Burst Communications, Part II: Upgrading Performance Doesn't Cost," *Military Electronics/Countermeasures* 8(9), 56-60 (September 1982).

## APPENDIX

Meteors approach the earth either in showers from known directions at certain times of the year, or sporadically, from random directions in the plane of the ecliptic. Since sporadic meteors are present at all times, they are generally the most useful. The approach velocities range between 11 and 72 km/s. The most probable lengths of the ionized trails are 15 to 25 km and occur at heights of 80 to 120 km. The initial radii of the trails range from a few meters at the higher altitudes to a fraction of a meter at the lower altitudes. Subsequently, the ions diffuse into the surrounding atmosphere with respective radial diffusion coefficients of about 140 to 1 m<sup>2</sup>/s.

Meteor trails are classified as underdense or overdense with respect to the degree of ionization of the trail. An electron line density of  $1-2.4 \times 10^{14}$  electrons/m is the generally accepted demarcation between underdense and overdense trails. The underdense trails, with electron line densities of approximately  $10^9$  to  $10^{14}$  electrons/m, are produced by meteors of radii between 8 microns and 0.04 cm, with masses from  $10^{-8}$  to  $10^{-3}$  grams. The overdense trails, with electron line densities of approximately  $10^{14}$  to  $10^{18}$  electrons/m, are produced by meteors of radii between 0.04 and 0.8 cm, with masses from 1 mg to 10 grams. Outside of these ranges, the smaller meteors produce negligible ionization and the larger meteors totally disintegrate in the upper atmosphere.

The lifetime of an underdense trail ranges from a small fraction of a second to a few seconds while that for an overdense trail ranges from a few seconds to the order of one minute (a lifetime of one hour is rare). The frequency of occurrence of sporadic meteor trails is, however, approximately inversely proportional to the electron line density, therefore underdense trails are the more useful in meteor burst communications. The time interval between occurrences of suitable meteor trails for meteor burst communications varies from seconds to minutes, with a mean of about twenty seconds. The diurnal variation in the number of meteor trails is about four to one with the maximum at approximately 6 AM and the minimum at approximately 6 PM local time. The yearly variation is roughly five to one with the maximum in July and the minimum in February in the northern hemisphere. Winds also effect trails with lifetimes greater than about one second. The distorted trails produce glints and fading and doppler frequencies as high as 18 Hz for a 50 MHz radar frequency.

The operating frequency for meteor burst communications ranges between 20 and 110 MHz. However, this range is generally restricted to 30 to 50 MHz for two reasons. First, the frequency must be higher than those which would be refracted from the various layers in the ionosphere, which would interfere with the burst communications. Second, the scattering cross section of a meteor trail varies inversely as the frequency, leading to a preference for low operating frequencies.